

Original Article

Negligible risk of surface transmission of SARS-CoV-2 in public transportation

Alina Pilipenco, MSc¹, Michala Forinová, MSc¹, Hana Mašková, MSc², Václav Hönig, PhD^{3,4}, Martin Palus, PhD^{3,4}, Nicholas Scott Lynn Jr., PhD¹, Ivana Višová, PhD¹, Markéta Vrabcová, MSc¹, Milan Houska, PhD¹, Judita Anthi, MSc¹, Monika Spasovová, MSc¹, Johana Mustacová, MSc², Ján Štěrba, PhD², Jakub Dostálek, PhD¹, Chao-Ping Tung, PhD⁵, An-Suei Yang, PhD⁵, Rachael Jack, PhD⁶, Alexandr Dejneka, PhD¹, Janos Hajdu, DSc^{6,7} and Hana Vaisocherová-Lísalová, PhD^{1,*}

¹Institute of Physics of the Czech Academy of Sciences, Na Slovance 2, 182 00 Prague, Czech Republic, ²Faculty of Science, University of South Bohemia, Branišovská 1645/31a, 370 05 České Budějovice, Czech Republic, ³Institute of Parasitology, Biology Centre of the Czech Academy of Sciences, Branišovská 31, 370 05 České Budějovice, Czech Republic, ⁴Department of Infectious Diseases and Preventive Medicine, Veterinary Research Institute, Hudcova 70, 621 00 Brno, Czech Republic, ⁵Genomics Research Center, Academia Sinica, 128 Academia Rd., Sec.2, Nankang Dist., Taipei 115, Taiwan, ⁶The European Extreme Light Infrastructure, ERIC, Za Radnici 835, 25241 Dolní Břežany, Czech Republic and ⁷Department of Cell and Molecular Biology, Uppsala University, Box 596, 751 24 Uppsala, Sweden

*To whom correspondence should be addressed. Email: lisalova@fzu.cz

Submitted 3 February 2023; Revised 14 April 2023; Editorial Decision 22 April 2023; Accepted 22 April 2023

Abstract

Background: Exposure to pathogens in public transport systems is a common means of spreading infection, mainly by inhaling aerosol or droplets from infected individuals. Such particles also contaminate surfaces, creating a potential surface-transmission pathway.

Methods: A fast acoustic biosensor with an antifouling nano-coating was introduced to detect severe acute respiratory syndrome coronavirus 2 (SARS-CoV-2) on exposed surfaces in the Prague Public Transport System. Samples were measured directly without pre-treatment. Results with the sensor gave excellent agreement with parallel quantitative reverse-transcription polymerase chain reaction (qRT-PCR) measurements on 482 surface samples taken from actively used trams, buses, metro trains and platforms between 7 and 9 April 2021, in the middle of the lineage Alpha SARS-CoV-2 epidemic wave when 1 in 240 people were COVID-19 positive in Prague.

Results: Only ten of the 482 surface swabs produced positive results and none of them contained virus particles capable of replication, indicating that positive samples contained inactive virus particles and/or fragments. Measurements of the rate of decay of SARS-CoV-2 on frequently touched surface materials showed that the virus did not remain viable longer than 1–4 h. The rate of inactivation was the fastest on rubber handrails in metro escalators and the slowest on hard-plastic seats, window glasses and stainless-steel grab rails. As a result of this study, Prague Public Transport Systems revised their cleaning protocols and the lengths of parking times during the pandemic.

Conclusions: Our findings suggest that surface transmission played no or negligible role in spreading SARS-CoV-2 in Prague. The results also demonstrate the potential of the new biosensor to serve as a complementary screening tool in epidemic monitoring and prognosis.

Key words: SARS-CoV-2, surface contamination, public transportation, Prague, antifouling biosensor, quartz crystal microbalance, qRT-PCR

Introduction

Public transportation is a significant factor in the spread of infectious diseases¹ mainly through aerosols, generated in confined spaces as people cough, sneeze and talk,^{2,3} and also by touching contaminated surfaces,^{4,5} followed by facial contact.^{6,7} Infections have been documented⁸ in subway trains, trams, buses, aircraft and cruise ships, including the spreading of *Mycobacterium tuberculosis*,^{9,10} influenza virus,¹¹ Middle East Respiratory Syndrome Coronavirus,¹² and severe acute respiratory syndrome coronavirus 2 (SARS-CoV-2).^{13–15} Transmission is modulated by various factors, including infectivity and virulence, crowd density, temperature, ventilation, humidity.^{16–18} Monitoring of pathogens (such as SARS-CoV-2) in public transportation helps keeping track of epidemics and aids the development of prognoses. Here we present a study on surface contamination by SARS-CoV-2 in the Prague Public Transport System, which operates metro, tram and bus services in the city.

Current methods for the analysis of surface swab samples are mainly based on the detection of viral genomic ribonucleic acid (vRNA) by quantitative reverse-transcription polymerase chain reaction (qRT-PCR) and its derived techniques.¹⁹ However, the sensitivity of qRT-PCR for swab samples is often reduced due to several factors, including high variation in sample composition, overall sample complexity and the presence of PCR inhibitors.^{20–22} qRT-PCR measurements detect the presence of vRNA fragments, and this is not directly correlated with infectivity.^{2,23,24} Recent advances in point-of-care (POC) methods offer possibilities to overcome some of the limitations of qRT-PCR measurements; surface-enhanced Raman spectroscopy, acoustic, colorimetric and surface plasmon resonance biosensors have shown a strong potential for rapid and sensitive pathogen detection in surface swab samples.^{25–27} Additionally, acoustic biosensors based on the quartz crystal microbalance (QCM) allow for the direct and label-free detection of specific pathogens.^{28–30} Here we used a new, antibody-based QCM biosensor, coated with an antifouling nano-layer, which provides a high degree of resistance to non-specific binding. We validate the use of this sensor technology for environmental samples and compare the results with results from the well-established qRT-PCR method for SARS-CoV-2 detection. For the label-free QCM biosensors as well as for any affinity-based direct detection formats, it is critical to mitigate the level of non-specific adsorption (fouling) by abundant biomolecules present in real-world biological samples, such as bodily fluids or crude surface swab samples. Fouling limits the ability to distinguish between specific and non-specific sensor signals, and can eventually block the sensor surface and thus impair the ability to capture the target. Antifouling surfaces that resist non-specific adsorption are currently one of the major research topics in POC biosensor research.

The paper covers four areas:

- (i) We describe a large-scale comparative study of the detection of SARS-CoV-2 in 482 surface swab samples collected

from multiple types of public-exposed surfaces in actively used buses, trams, metro trains and metro platforms in the City of Prague. **Figure 1** shows the sampling points in the Prague Public Transport System.

- (ii) We describe the use of a fast biosensor for these measurements in tandem with conventional qRT-PCR measurements.
- (iii) We present results from cell culture assays to evaluate the replication ability of SARS-CoV-2 from positive surface samples.
- (iv) Finally, we show data on the rate of the decay of SARS-CoV-2 on frequently touched surface materials.

Materials and methods

Surface swab sample collection from public transportation

We collected 482 surface swabs from various exposed surfaces in trams, buses, metro trains and platforms. Each swab sample covered an area of 225 cm² and samples were collected into 1 ml of phosphate-buffered saline (PBS) using certified swab kits and a standard world health organization (WHO)-approved protocol.³² These liquid swab samples were analysed using both our new antifouling biosensor and the conventional qRT-PCR technique. *Supplementary Data* details the specific protocol used for sample collection, the qRT-PCR method used and details of each sample (**Tables S1–S4**). The results of both methods (biosensor and qRT-PCR) were evaluated independently and met the parameters of the randomized, double-blind study. Samples that showed positivity for the SARS-CoV-2 from one or the other method were subsequently subjected to a culture test to verify the viability of the virus and the possible infectivity of the sample. Samples were collected between 7 and 9 April 2021 in the middle of the lineage Alpha SARS-CoV-2 epidemic wave. We analysed 160 nucleotide sequences available in the GISAID database³³ (EPI_SET_230322fw) from patient samples collected in Prague during the period of 31.3.2021–16.4.2021, spanning a week before and a week after the sampling date (7–9 April 2021). Results with the Pangolin COVID-19 Lineage Assigner³⁴ show that 95.63% of all infections in Prague were caused by the B.1.1.7 Alpha lineage in this period. Minor components were the B.1.1.318 lineage (1.88%), the B.1.258 lineage (1.25%), the B.1.351 Beta lineage (0.63%) and the B.1.617.1 Kappa lineage (0.63%).

Fast label-free biosensor measurements

We have developed a fast QCM-based acoustic biosensor³⁵ (**Figure 2**) with improved antifouling properties for ultra-sensitive direct detection of viruses and other pathogens in crude, untreated samples (see also *Supplementary Data*). The sensor surface was coated with an antifouling biorecognition coating,

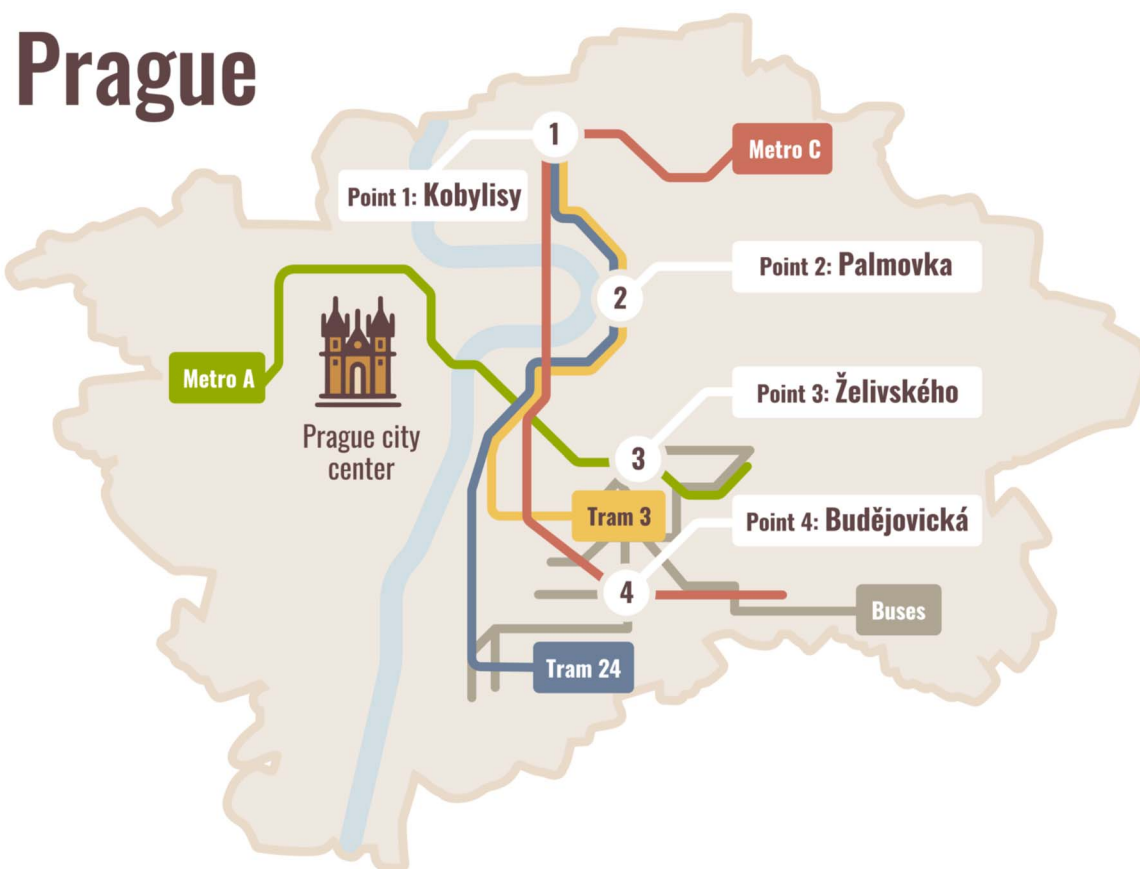


Figure 1. Sampling sites at the most crowded points of the Prague Public Transport System. Swab samples were collected on 7–9 April 2021, during one of the local peaks of the COVID-19 pandemic in the Czech Republic when ~5000 new cases of SARS-CoV-2 infections were detected daily, and the overall number of infected people reached ~80 000 in the country. At the time of the sampling, one in 240 people were documented as COVID-19 positive³¹

which contained an antibody-functionalised terpolymer brush (Figure 2). We used this sensor to test the complex surface swab samples. All measurements with the biosensor were performed in parallel with conventional but slower qRT-PCR measurements.

Our antifouling biosensor combines the latest developments in tailored biorecognition elements with a fast, simple, portable, cheap and ready-to-use QCM detection technique, offering analysis times of <20 min. Before field deployment, the analytical performance of the QCM biosensor was determined from the analysis of a large test sample set (Figures S4 and S5). QCM crystals were modified with the terpolymer brush and pre-functionalized with antibodies reactive towards the nucleocapsid (N) protein of the virus. Each sample was analysed in duplicate by the antifouling biosensor. As seen in Figure S4, for each QCM channel, we used a measurement scheme consisting of (i) the injection of negative control (undiluted cell culture void of SARS-CoV-2 but full of other proteins and cells) to verify the antifouling behaviour of the terpolymer brush, (ii) sequential injections of three randomly selected surface swab samples, done to maximize measurement throughput and (iii) the injection of positive control (undiluted cell culture sample containing 10^4 PFU/ml of SARS-CoV-2) to verify the biorecognition activity. The signal response was calculated from the sensor response in the PBS buffer before and after the application of the sample (Figure S4).

QCM data analysis was performed using the software Origin version 2020b (OriginLab Corporation, Massachusetts, USA). For comparison of groups, we utilized the Mann–Whitney U test. MaxStat Pro 3.6 software (MaxStat Software, Cleverns, Germany) and SigmaPlot 13 (Systat Software, Palo Alto, CA, USA) were used to perform all statistical analyses.

Samples recognized as positive by both the antifouling biosensor and qRT-PCR and a set of samples recognized as positive by one of the methods and borderline positive by the other, underwent cell culture experiments to detect the presence of replicating (infectious) virus; details of these experiments can be found in the *Supplementary Data*.

Measurement of the decay of the virus on exposed surface materials in the public transport system

Surface materials were characterized by their ability to maintain the activity of SARS-CoV-2. We used the SARS-CoV-2 strain hCoV-19/Czech Republic/951/2020, GISAID ID: EPI_ISL_414477, isolated from a clinical sample from Ústí nad Labem at The National Institute of Public Health Centre for Epidemiology and Microbiology in Prague (see *Supplementary Data*). Virus samples of standard concentration, 2×10^5 PFU/ml, were applied to decontaminated sample materials from the

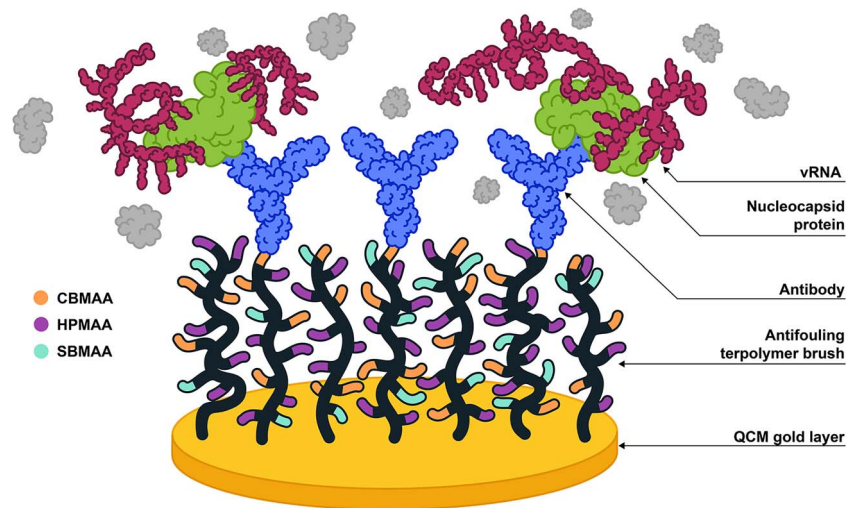


Figure 2. Schematic view of the detector surface of the acoustic biosensor chip with antifouling terpolymer layer.³⁵ This sensor chip was used in a QCM for the rapid detection of the SARS-CoV-2 N protein (green). vRNA is shown in dark red. The sensors were used in a single-step label-free assay to detect the SARS-CoV-2 N protein. The terpolymer brush structure offers antifouling properties and is made up by carboxybetaine methacrylamide (CBMAA orange), *N*-(2-hydroxypropyl) methacrylamide (HPMAA purple) and sulfobetaine methacrylamide (SBMAA turquoise) components. These brushes were functionalised with tailored antibodies (blue) against the SARS-CoV-2 N protein. The specificity of the sensor can be changed by changing the antibodies, and this offers versatility. Further details about the sensor are given in [Supplementary Figures S1–S5](#)

Prague Public Transport System (70% ethanol for 10 min, ultraviolet light 30 min), including glass, stainless steel, plastic, rubber and various other highly exposed materials. After 1, 2 and 4 h, following virus deposition, the surfaces were washed with 20 μ l of Vero-E6 culture medium and used directly for plaque titration in a 96-well format as described previously.³⁵ Experiments were performed in duplicate. The number of plaques was counted and the viral titre expressed as the number of PFU/ml of the sample and compared to the control. For more details, see *Supplementary Data*.

Results and discussion

Decay of SARS-CoV-2 on various surface materials used in public transport vehicles and stations

We measured the rate of decay of the virus on frequently touched surfaces in public transport vehicles and metro stations. This included tram windows, painted grab rails in older public transport vehicles, stainless steel grab rails in newer models, rubber handrails of escalators in metro stations, plastic tram seats, plastic buttons for door opening in modern trams and the different door opening buttons from older models (for a selection of these materials see [Figure 3](#)).

We observed a gradual decrease in the number of replicating/infectious virus particles over time on all surfaces tested ([Figure 3A](#)). After 1 h, there were statistically significant decreases in viral titre for all surfaces [analysis of variance $P < 0.01$ ([Table S5](#))], and after 4 h, the titre dropped to the detection limit of the method in all samples, suggesting that after 4 h, the risk of infection was minimal, although still non-zero. The fastest drop in infectivity was observed on the rubber handrails of metro escalators (less than an hour), whilst the slowest decays were measured on the painted and stainless-steel grab rails of metro cars and trams, on window glasses and on

the hard-plastic seats of trams (<4 h). This agrees with other studies, showing that the virus can remain viable longer on certain surfaces, including metals and plastics.^{2,6}

Surface contamination measurements by qRT-PCR and the QCM-based antifouling biosensor

In our study to assess the risk of encountering SARS-CoV-2 on surfaces that people frequently touch in the Prague Public Transport System, we used two independent measurement methods based on different detection principles on all samples. We collected a total of 482 surface swab samples from exposed surfaces in trams, buses, metro vehicles and metro platforms. All samples were tested for the presence of SARS-CoV-2 by qRT-PCR and by our rapid biosensor in a double-blind study. Sample collections were performed between 7 and 9 April during the morning rush hours (from 8 to 10 a.m.) when the load on the transport system was the highest. There was no lockdown in Prague during the sampling period. The surface swabs varied in viscosity, chemical composition, pH and ionic strength. Samples were collected from some of the busiest vehicles and routes in the local public transit system, crossing through the most crowded places in Prague ([Figure 1](#)). These places are located near or serve important Prague hospitals and other medical facilities. Samples were either collected during the full operation of the transport system (e.g. from metro stations) or immediately after the exit of passengers from vehicles at the end stations (e.g. samples from various cars). Surface swabs from buses were collected at the Želivského interchange near the University Hospital Královské Vinohrady, where six bus lines intersect (see *Supplementary Data*) and important Prague hospitals and polyclinics are located (the University Hospital Královské Vinohrady and Thomayer University Hospital and the polyclinics of Vršovice, Malešice, Zahradní město, Budějovická, Nuselská, Modřany, Spořilov, Háje, Uhřetěves and Zelený pruh). Sampling of surfaces

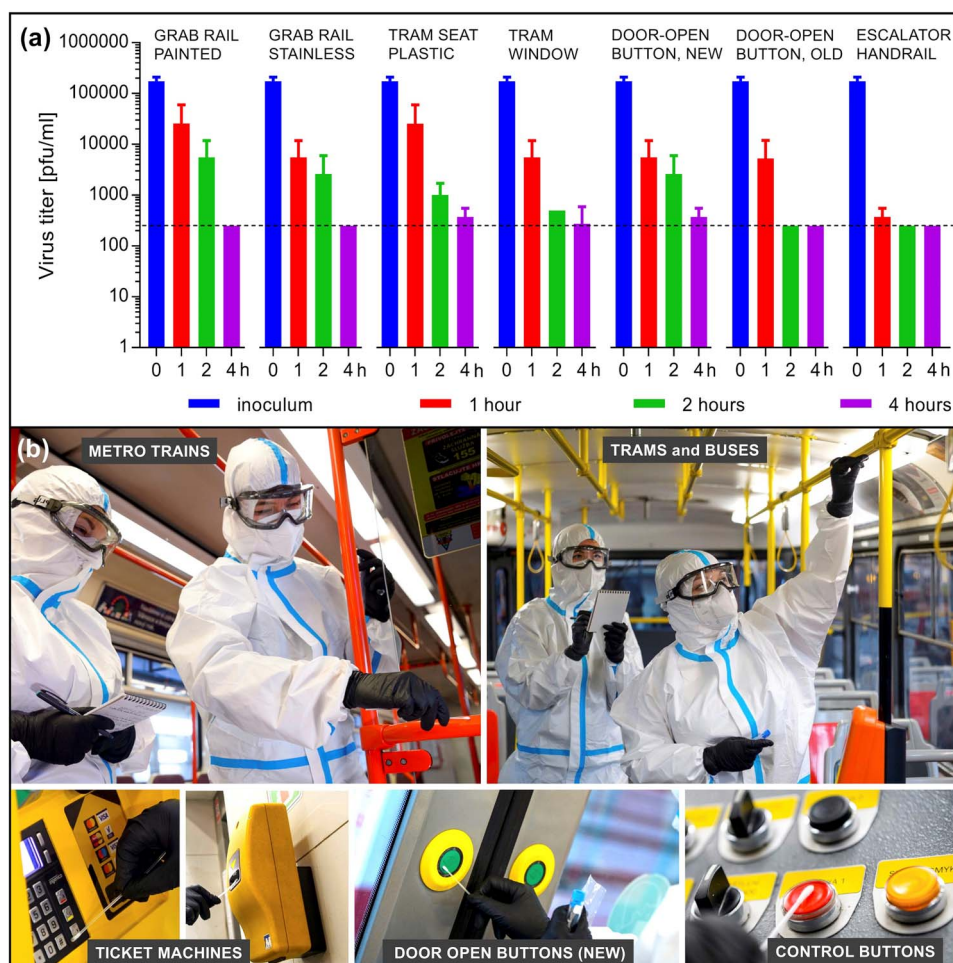


Figure 3. (a) The rate of decay of the SARS-CoV-2 virus on various exposed surfaces in public transport vehicles and stations in Prague. Measurements were made on surface samples in the laboratory. Virus titre represents the concentration of replicating infectious virus particles as determined by the plaque assay (Materials and methods). Time 0 corresponds to the virus titre of the inoculum. The titre was checked in surface swabs after 1, 2 and 4 h following the application of the inoculum onto the surface. The horizontal dashed line indicates the detection limit of the method. All measurements were performed and analysed in duplicate (see *Supplementary Data*). (b) Images of some of the areas from where surface swabs were taken during 7–9 April 2021. Sampling included a wider range of surface materials than those characterized in (a). For further details see *Supplementary Data*. With permission by the Prague Public Transit Company. Photographs by Petr Hejna

from the metro system took place at the Želivského stop, which belongs to metro line A that runs through the whole of Prague and starts at Hospital Motol. This metro line also passes through the tourist centre of Prague as well as station Nádraží Veleslavin, which connects to the bus line, serving the main international airport of Prague. Other collection points were set up on metro line C at the Kobylysy and Budějovická stops (Figure 1). This metro line runs through crowded central stops and through the international bus station at Florenc and the Central Railway Station of Prague. Surface swabs from trams were collected at the final stop of Vozovna Kobylysy for lines 3 and 24, whose route goes through the entire city centre from the south/southeast to the north. These lines serve large healthcare facilities such as The General Teaching Hospital in Prague, Bulovka Hospital, Institute for Mother and Child Care and the Municipal polyclinic of Prague. Figure 4 shows the number of passengers transported on working days by the metro system of Prague during 2020, and 2021, and indicates the time of the sampling campaign.

qRT-PCR analyses of the samples required RNA extraction, and were performed for the envelope (E) protein, N protein and RNA-dependent RNA polymerase (RdRP) coding genes. These qRT-PCR measurements gave 23 positive results for at least one of the three marker genes. Only two samples were found to be positive for all three genes and thus were considered unambiguously positive by qRT-PCR (Table 1). This number of positive samples represents only 0.4% of the total number of tested samples. A total of 21 samples (4.4% of the total of 482 samples) were considered borderline positive by qRT-PCR, i.e. exhibiting positive response in one or two tested gene sequences. In comparison, the antifouling biosensor identified 10 samples (2.1%) as unambiguously positive (no samples were classified by the antifouling biosensor as borderline-positive samples). The complete list of positive and borderline-positive samples identified by both methods is shown in Table 1. The table also highlights an excellent correlation between the positive and borderline-positive results from the two completely different methods. When considering all 482 samples, the agreement of

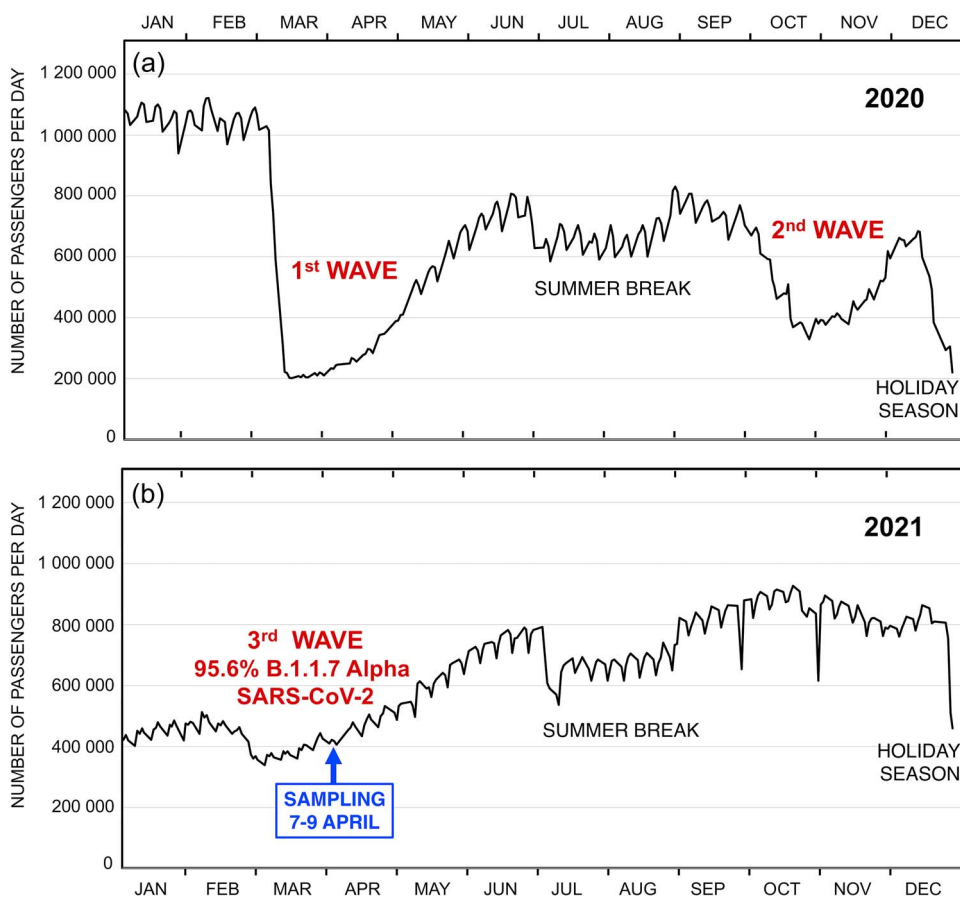


Figure 4. Passenger numbers on working days in the Prague metro during the COVID-19 pandemic in 2020 (a) and 2021 (b).³⁶ Data for both years span the period of 8 January to 30 December. Under normal conditions, the metro carries ~1–1.1 million passengers per day. The sudden drop of passenger numbers in March 2020 shows the onset of the first wave of the pandemic. From the end of April 2020, passenger numbers gradually increased and stabilized at ~600 000 passengers per day. The onset of the second wave of the pandemic is indicated by a decrease in passenger numbers during October 2020. The third wave arrived in February–March 2021, followed by a slow recovery, extending into October 2021. Samples used in this paper were collected between 7 and 9 April 2021 in the middle of the lineage Alpha SARS-CoV-2 epidemic wave. During this period, most of the infections (95.63%) were caused by the B.1.1.7 Alpha lineage in Prague, with minor components from lineages B.1.1.318 (1.88%), B.1.258 (1.25%), B.1.351 Beta (0.63%) and B.1.617.1 Kappa (0.63%). At the time of the sample collection between 7 and 9 April 2021, one in 240 people were COVID-19 positive in Prague³¹

measurements was 98% (positives and negatives). There was no correlation between the detection of coronavirus and the origin of samples (bus, tram, metro, metro platforms), that is, detection of the virus did not depend on the type of public transport and is the same for all vehicle types tested (Table S6). Considering the quantitative SARS-CoV-2 detection by the antifouling biosensor, we found that the sensor response to positive samples was in the range of -6.3 to -16.1 Hz (see Figure S4). Considering the sensor calibration curve reported previously³⁵ such sensor responses correspond to virus concentrations of $\sim 10^4$ PFU/ml.

qRT-PCR measurements identified two positive samples out of the 482 samples collected. qRT-PCR also identified 21 ‘borderline positive’ samples. The QCM-based antifouling biosensor found 10 positive samples. Table 1 shows that nine of the 10 positive results by the antifouling biosensor match the positive/borderline qRT-PCR results. The positive samples identified by the antifouling biosensor with code numbers 5.2, M1 and M65 in Table 1 were classified as borderline positive by qRT-PCR. Moreover, four positive samples identified by the antifouling biosensor were collected from places near surfaces from

where qRT-PCR measurements gave borderline-positive results (e.g. from the same part of the car, see also Tables S7 and S8 in Supplementary Data). Samples 9.11, 10.2, M54 and M92 were collected near samples 9.5, 10.3, M51 and M96, respectively. These samples were evaluated as borderline positive by the qRT-PCR method. It is likely that these co-localized samples come from the same virus carrier(s). Only one sample classified as positive by antifouling biosensor (H6) was not confirmed by qRT-PCR. This could be due to (a) low RNA concentration (highly degraded RNA but well preserved protein), (b) inhibition of qRT-PCR by an inhibitor in the surface swab sample, (c) detection of the N protein of a closely related virus by the antifouling biosensor. We note that there were no false negatives in the assignments based on results from the antifouling biosensor.

Previous studies addressing SARS-CoV-2 in public transportation and related environments in air and surface samples reported results with high variability in the prevalence of positive samples (0–42% for surface, 0–67% for air samples) (summarized in Table S11). Our results on surfaces samples belong to the bottom part of this spectrum (2–5% of positive surface

Table 1. List of surface swab samples identified as positive by the antifouling biosensor and positive or borderline positive by qRT-PCR. For details of sampling sites and sample codes, see Supplementary Tables S1–S4. Statistical data on the measurements are given in Supplementary Tables S5–S10

| Positive Samples qRT-PCR | Positive Samples Biosensor | Borderline-Positive qRT-PCR |
|---|--|---|
| Samples from identical sampling points: | | |
| 11.6 | 11.6 | |
| Bus no. 11, seat handle | Bus no. 11, seat handle | |
| 31 | 31 | |
| Metro platform lift buttons | Metro platform, lift buttons | |
| | 5.2 | 5.2 |
| | Bus no. 5, door glass | Bus no. 5, door glass |
| | M1 | M1 |
| | Metro car no. 1, door-open button | Metro car no. 1, door-open button |
| | M65 | M65 |
| | Metro car no. 11, vertical handrail | Metro car no. 11, vertical handrail |
| Samples from nearby sampling points: | | |
| | 10.2 | 10.3 |
| | Bus no. 10, door glass | Bus no. 10, door handle |
| | 9.11 | 9.5 |
| | Bus no. 9, button no. 2 | Bus no. 9, upper horizontal handrail |
| | M54 | M51 |
| | Metro car no. 9, upper horizontal handrail | Metro car no. 9, door glass |
| | M92 | M96 |
| | Metro car no. 16, door handle | Metro car no. 16, upper horizontal handrail |
| Unrelated positive/borderline-positive samples: | | |
| | H6 | 5.4, 7.6, 10.7, 12.8, C9.2, G8, J9, L9, T4, 33, M7, M13, M14, M81 |

For a full list of samples, see Supplementary Tables S1–S4.

The bold values in Table 1 represent sample codes. All sampling sites and sample codes are listed in Supplementary Tables S1–S4.

samples). Studies comparing surface and air samples collected in the same environment usually report significant differences in SARS-CoV-2 RNA prevalence between air and surface samples. Nevertheless, some authors report higher prevalence in surface swabs,^{15,37,38} others in air samples³⁹ and others similar prevalence rates for both.^{40,41} The reasons for this as well as for the overall variability could be (amongst others) related to differences in sampling and detection methods and the tools used, as well as to the intensity of public transport use, the actual COVID-19 incidence, properties of the currently circulating strains, environmental conditions and cleaning and disinfection procedures.^{42,43}

Tests on the viability of SARS-CoV-2 in positive swab samples

Two samples (11.6, 31) were recognized as unambiguously positive by both antifouling biosensor and qRT-PCR. Another eight samples were identified by the antifouling biosensor as positive (Table 1). All of these samples were subjected to a culture assay on Vero E6 cells (sensitive to SARS-CoV-2 infection). Two of the 10 samples (11.6, L9) elicited a massive cytopathic effect immediately after inoculation. These samples were filtered through a bacteriological filter and transferred to new cells with fresh media. Nevertheless, the cytopathic effect was observed again, indicating a cytotoxic compound in the swab, possibly a disinfectant. No cytopathic effect was observed in any of the remaining samples. qRT-PCR results were negative for all samples after 3, 6 and 9 days following inoculation, except for the positive control. No replication of the SARS-CoV-2 was detected in any of the samples.

The airborne route of transmission is considered epidemiologically the most relevant.^{44,45} Given the infrequent detection of infectious virus on surfaces in public environments (this study, Table S11) and the estimated infectious dose,⁴⁶ we can assume that contaminated surfaces play a minor role in the spread of disease.⁴⁷ Nevertheless, detection of viral RNA in surface samples can be used as an indicator of past air contamination.^{47–49} It can also be used for the direct monitoring of environmental contamination, and for the analysis of currently circulating variants. In addition, surface sampling may be more effective because it does not require specialized technical equipment and the prevalence of positive surface samples is generally higher than in air samples collected in the same both environment, although there is great variability amongst the studies and the air sampling techniques used (Table S11). On the other hand, detection of the virus in air is more closely related to the actual risk of infection. The detection of infectious virus in qRT-PCR positive surface or air samples is relatively scarce from environmental surface and air samples (Table S11). The virus is inactivated in a rate depending on numerous factors^{6,42,50,51} but viral RNA is significantly more stable.⁵² Vass *et al.*⁵³ reported a ratio of 1:10 between the number of infectious virus particles and copies of viral RNA genomes in cell culture positive samples both for surface swabs and for aerosol samplers. Apart from virus inactivation caused by environmental factors, further loss of viable virus might be associated with inactivation during the sampling procedure, and/or decreased recovery of the virus from the sampled material or from the matrix of sampling tools (air filters, swabs, etc.), possibly producing false negative results.^{54,55}

Possible limitations of the study

Possible limitations of our study may lie in the sampling phase: there is a huge diversity in the surface materials that are used in public transport environments, some of them might be difficult to sample due to high porosity or other features causing low recovery of the virus.⁵⁶ Therefore, multiple parts of the transportation system and different surfaces, often next to each other, were sampled in our study.

The amount of viral RNA present on surfaces in public transportation might be highly variable (16–10⁵ genome copies/m²; Table S11), and therefore some samples might be false negative due to not reaching the detection limit of the two methods. To overcome this risk, we have sampled a fairly large area and we have used two independent methods for virus detection. The results (minor inconsistencies between the two methods and failed amplification of one or two of the gene targets) indicate that some samples contained a viral (RNA) load close to the detection limit of the methods.

Furthermore, the COVID-19 pandemic is associated with frequent changes of the major genetic variants. Nevertheless, the qRT-PCR as well as the biosensor method were so far able to detect all the major variants of the virus. Furthermore, the qRT-PCR method used for detection, amplifies three independent gene targets simultaneously, hence the method and its combination with the antibody-based biosensor detection are quite robust against changes in the genome of SARS-CoV-2.

Because the samples were collected in the middle of Alpha SARS-CoV-2 epidemic wave (B.1.1.7 in 95.63% of patient sequences), we can assume that most of the positive results are the same variant. No significant differences in the infectivity of the virus after exposure to the environment were found when comparing the Alpha variant to other variants of concern⁵¹ including Omicron.⁵⁷ On the other hand, some variants were previously reported to have increased infectivity in general, which can be associated with numerous factors such as higher viral loads in patients, prolonged virus shedding, but also a more effective receptor binding, immune evasion, faster replication, or possibly a lower infectious dose.⁵⁸ Therefore, a similar degree of environmental contamination with one variant may result in a significantly different risk of infection than with another, and thus the results should be interpreted with regard to the currently circulating variants.

Conclusions

Results of this work show that surface contamination of public transport vehicles by SARS-CoV-2 in Prague was at a very low level at the height of the pandemic in 2021. Out of 482 swab samples taken in public transport vehicles and metro stations, only 10 were deemed positive, and none of the positive samples contained active SARS-CoV-2, capable of infection and replication in Vero E6 cells.

We introduced a fast, acoustic biosensor, developed in the collaboration²⁸ for the direct and label-free specific detection of SARS-CoV-2. The sensor provided results directly from surface swabs in ~20 min. The surface of the sensor chip was coated with an antifouling antibody-functionalised terpolymer brush to bind the N protein of the virus, and measurements were performed in a portable QCM. Measurements with this sensor agree well with

results from duplicate measurements with the slower and more elaborate qRT-PCR technique. The results from this large-scale study highlight the abilities of the new-generation antifouling biosensor for rapid measurements in complex surface swab samples without the need for sample pre-treatment or filtering. The specificity of the biosensor can be altered by attaching different antibodies to the sensor surface.^{28–30} The sensor has the potential to serve as a complementary screening tool in epidemic monitoring and prognosis.

Additional studies on the decay of the SARS-CoV-2 on frequently touched surface materials showed that SARS-CoV-2 did not survive longer than ~1–4 h on any of the common surface materials used in the Prague Public Transport System. The fastest inactivation rate was on samples from the rubber escalator railings (<1 h to reach the detection limit), and the slowest on glass, stainless steel and hard-plastic surfaces (2–4 h).

Information from this study has been implemented in the operational strategy of the Prague Public Transport System to optimize cleaning protocols and the lengths of parking times before the next journey.

Supplementary data

Supplementary data are available at *JTM* online.

Funding

This work was supported by Praemium Lumina Quaeruntur grant of the Czech Academy of Sciences (LQ100101902) to HVL, the Czech Science Foundation (contract # 21-19779S) to HVL, the project Biosensors for sustainable industrial production, BIOSIP (n. CZ.01.1.02/0.0/0.0/20_321/0024852) to HVL (Co-PI) and ELIBIO (No. CZ.02.1.01/0.0/0.0/15_003/0000447) from the European Regional Development Fund to JH.

Acknowledgments

The authors thank Jan Weber, Institute of Organic Chemistry and Biochemistry of the Czech Academy of Sciences, Prague, Czech Republic, for providing the SARS-CoV-2 coronavirus isolate; Petra Straková, Veterinary Research Institute, Brno, Czech Republic, for the initial propagation of SARS-CoV-2; Dopravní podnik hl. m. Prahy for their support and collaboration on this study; Adam Frtús, Barbora Smolková, Maria Uzhytchak, Kateřina Mrkvová, Michala Drahošová and Nicola Poledňáková from the Institute of Physics of the Czech Academy of Sciences for their participation in the surface swab samples collection; Oleg Lunov for his help with statistical data analysis; Marek Piliarik, Institute of Photonics and Electronics CAS, Prague, Czech Republic, for his critical assessment and advices on the work presentation; Daniel Špaček and Mikhail Koreshkov for their help with the graphic design; the Prague Public Transit Company and Petr Hejna for providing photos for Figure 3b.

Author's contribution

Alina Pilipenco (Data curation [Lead], Investigation [Equal], Methodology [Equal], Writing—original draft [Lead]), Michala Forinová (Data curation [Equal], Project administration [Equal], Writing—review & editing [Equal]), Hana Mašková (Data curation [Equal]), Václav Hönig (Data curation [Equal]),

Martin Palus (Data curation [Equal]), Nicholas Scott Lynn Jr (Writing—review & editing [Equal]), Ivana Víšová (Data curation [Equal]), Markéta Vrabcová (Data curation [Equal]), Milan Houska (Data curation [Supporting]), Judita Anthi (Data curation [Equal]), Monika Spasovová (Data curation [Supporting]), Johana Mustacová (Data curation [Supporting]), Ján Štěrba (Data curation [Equal]), Jakub Dostálek (Writing—review & editing [Equal]), Chao-Ping Tung (Data curation [Equal]), An-Suei Yang (Data curation [Equal]), Rachael Jack (Conceptualization [Equal], Writing—review & editing [Equal]), Alexandr Dejneka (Project administration [Equal], Supervision [Equal]), Janos Hajdu (Conceptualization [Equal], Writing—review & editing [Equal]) and Hana Vaisocherová—Lísalová (Conceptualization [Lead], Supervision [Equal], Writing—review & editing [Equal])

Availability of data and materials

Supplementary Data are available for this paper online.

Conflict of interest

The authors declare that they have no competing interests.

Ethics approval and consent to participate

Not applicable.

Meetings at which the paper has been presented

None.

References

- Afshinnekoo E, Meydan C, Chowdhury S *et al.* Geospatial resolution of human and bacterial diversity with city-scale metagenomics. *Cell Syst* 2015; 1:72–87. <https://doi.org/10.1016/j.cels.2015.01.001>.
- Wölfel R, Corman VM, Guggemos W *et al.* Virological assessment of hospitalized patients with COVID-2019. *Nature* 2020; 581:465–9. <https://doi.org/10.1038/s41586-020-2196-x>.
- Dhama K, Khan S, Tiwari R *et al.* Coronavirus disease 2019 - COVID-19. *Clin Microbiol Rev* 2020; 33:e00028–0. <https://doi.org/10.1128/CMR.00028-20>.
- Klompas M, Baker MA, Rhee C. Airborne transmission of SARS-CoV-2: theoretical considerations and available evidence. *JAMA* 2020; 324:441–2. <https://doi.org/10.1001/jama.2020.12458>.
- Hickey JLS, Reist PC. Health significance of airborne microorganisms from wastewater treatment processes part II: health significance and alternatives for action. *J Water Pollut Control* 1975; 47:2758–73.
- Doremalen N, Bushmaker T, Morris DH *et al.* Aerosol and surface stability of SARS-CoV-2 as compared with SARS-CoV-1. *N Engl J Med* 2020; 382:1564–7. <https://doi.org/10.1056/NEJMc2004973>.
- Zhao Y, Richardson B, Takle E *et al.* Airborne transmission may have played a role in the spread of 2015 highly pathogenic avian influenza outbreaks in the United States. *Sci Rep* 2019; 9:11755. <https://doi.org/10.1038/s41598-019-47788-z>.
- Zhao B, Dewald C, Hennig M *et al.* Microorganisms @ materials surfaces in aircraft: potential risks for public health? – a systematic review. *Travel Med Infect Dis* 2019; 28:6–14. <https://doi.org/10.1016/j.tmaid.2018.07.011>.
- Feske ML, Teeter LD, Musser JM, Graviss EA. Giving TB wheels: public transportation as a risk factor for tuberculosis transmission. *Tuberculosis* 2011; 91:S16–23. <https://doi.org/10.1016/j.tube.2011.10.005>.
- Andrews JR, Morrow C, Wood R. Modeling the role of public transportation in sustaining tuberculosis transmission in South Africa. *Am J Epidemiol* 2013; 177:556–61. <https://doi.org/10.1093/aje/kws331>.
- Mangili A, Gendreau MA. Transmission of infectious diseases during commercial air travel. *Lancet* 2005; 365:989–96. [https://doi.org/10.1016/S0140-6736\(05\)71089-8](https://doi.org/10.1016/S0140-6736(05)71089-8).
- Tang JW, Wilson P, Shetty N, Noakes CJ. Aerosol-transmitted infections—a new consideration for public health and infection control teams. *Curr Treat Options Infect Dis* 2015; 7:176–201. <https://doi.org/10.1007/s40506-015-0057-1>.
- Abrahão JS, Sacchetto L, Rezende IM *et al.* Detection of SARS-CoV-2 RNA on public surfaces in a densely populated urban area of Brazil: a potential tool for monitoring the circulation of infected patients. *Sci Total Environ* 2021; 766:142645. <https://doi.org/10.1016/j.scitotenv.2020.142645>.
- Moriarty LF, Marston BJ, *et al.* Public health responses to COVID-19 outbreaks on cruise ships — worldwide, February–March 2020. In: *Wkly MMM*, 2020:347–52. <http://dx.doi.org/10.15585/mmwr.mm6912e3>.
- Moreno T, Pintó RM, Bosch A *et al.* Tracing surface and airborne SARS-CoV-2 RNA inside public buses and Subway trains. *Environ Int* 2021; 147:106326. <https://doi.org/10.1016/j.envint.2020.106326>.
- Baker RE, Mahmud AS, Wagner CE *et al.* Epidemic dynamics of respiratory syncytial virus in current and future climates. *Nat Commun* 2019; 10:5512. <https://doi.org/10.1038/s41467-019-13562-y>.
- Chu DK, Akl EA, Duda S *et al.* Physical distancing, face masks, and eye protection to prevent person-to-person transmission of SARS-CoV-2 and COVID-19: a systematic review and meta-analysis. *Lancet* 2020; 395:1973–87. [https://doi.org/10.1016/S0140-6736\(20\)31142-9](https://doi.org/10.1016/S0140-6736(20)31142-9).
- Yan EL, Yam. Climate change and the origin of SARS-CoV-2. *J Travel Med* 2020; 27:taaa224. <https://doi.org/10.1093/jtm/taaa224>.
- Vandenberg O, Martiny D, Rochas O, van Belkum A, Kozlakidis Z. Considerations for diagnostic COVID-19 tests. *Nat Rev Microbiol* 2021; 19:171–83. <https://doi.org/10.1038/s41579-020-00461-z>.
- Iglói Z, Ieven M, Abdel-Karem Abou-Nouar Z *et al.* Comparison of commercial realtime reverse transcription PCR assays for the detection of SARS-CoV-2. *J Clin Virol* 2020; 129:104510. <https://doi.org/10.1016/j.jcv.2020.104510>.
- Basso D, Aita A, Navaglia F *et al.* SARS-CoV-2 RNA identification in nasopharyngeal swabs: issues in pre-analytics. *Clin Chem Lab Med* 2020; 58:1579–86. <https://doi.org/10.1515/cclm-2020-0749>.
- Xie X, Zhong Z, Zhao W *et al.* Chest CT for typical coronavirus disease 2019 (COVID-19) pneumonia: relationship to negative RT-PCR testing. *Radiology* 2020; 296:E41–5. <https://doi.org/10.1148/radiol.2020200343>.
- Bullard J, Dust K, Funk D *et al.* Predicting infectious severe acute respiratory syndrome coronavirus 2 from diagnostic samples. *Clin Infect Dis* 2020; 71:2663–6. <https://doi.org/10.1093/cid/ciaa638>.
- Hong K, Cao W, Liu Z *et al.* Prolonged presence of viral nucleic acid in clinically recovered COVID-19 patients was not associated with effective infectiousness. *Emerg Microbes Infect* 2020; 9:2315–21. <https://doi.org/10.1080/22221751.2020.1827983>.
- He L, Chen T, Labuza TP. Recovery and quantitative detection of Thiabendazole on apples using a surface swab capture method followed by surface-enhanced Raman spectroscopy. *Food Chem* 2014; 148:42–6. <https://doi.org/10.1016/j.foodchem.2013.10.023>.
- Alamer S, Eissa S, Chinnappan R *et al.* Rapid colorimetric Lactoferrin-based sandwich immunoassay on cotton swabs for the detection of foodborne pathogenic bacteria. *Talanta* 2018; 185:275–80. <https://doi.org/10.1016/j.talanta.2018.03.072>.
- Ashley J, Piekarska M, Segers C *et al.* An SPR based sensor for allergens detection. *Biosens Bioelectron* 2017; 88:109–13. <https://doi.org/10.1016/j.bios.2016.07.101>.

28. Forinova M, Pilipenco A, Visova I *et al.* Biosensor for rapid detection of SARS-CoV-2 in real-world samples. *IEEE Sensor* 2021; 1–4. <https://doi.org/10.1109/Sensors47087.2021.9639783>.
29. Wang R, Li Y. Hydrogel based QCM Aptasensor for detection of avian Influenzavirus. *Biosens Bioelectron* 2013; 42:148–55. <https://doi.org/10.1016/j.bios.2012.10.038>.
30. Wachiralurpan S, Phung-On I, Chanlek N *et al.* In-situ monitoring of real-time loop-mediated isothermal amplification with QCM: detecting listeria monocytogenes. *Biosensors* 2021; 11:308. <https://doi.org/10.3390/bios11090308>.
31. Komenda M, Karolyi M, Bulhart V, Žofka J, Brauner T, Hak J, *et al.* Onemocnění Aktuálně. COVID-19: overview of the current situation for the capital city of Prague. *Ministry of Health of The Czech Republic*. 2022. <https://onemocneni-aktualne.mzcr.cz/covid-19>.
32. World Health Organization. Diagnostic testing for SARS-CoV-2: interim guidance, 11 September 2020. World Health Organization, 2020. <https://apps.who.int/iris/handle/10665/334254>.
33. Shu Y, McCauley J. GISAID: global initiative on sharing all influenza data – from vision to reality. *Eurosurveillance* 2017; 22:30494. <https://doi.org/10.2807/1560-7917.ES.2017.22.13.30494>.
34. Ai O'Toole E, Scher E, Underwood A *et al.* Assignment of epidemiological lineages in an emerging pandemic using the pangolin tool. *Virus Evol* 2021; 7:veab064. <https://doi.org/10.1093/ve/veab064>.
35. Forinová M, Pilipenco A, Víšová I *et al.* Functionalized terpolymer-brush-based biointerface with improved antifouling properties for ultra-sensitive direct detection of virus in crude clinical samples. *ACS Appl Mater Interfaces* 2021; 33:60612–624. <https://doi.org/10.1021/acsami.1c16930>.
36. *Dopravní podnik hl. m. Prahy. Prague Transportation Yearbook 2021*. Prague: Technická správa komunikací hl. m. Prahy (TSK), 2021. <https://www.tsk-praha.cz/static/udi-rocenka-2021-cz.pdf>.
37. Hoffman JS, Hirano M, Panpradist N *et al.* Passively sensing SARS-CoV-2 RNA in public transit buses. *Sci Total Environ* 2022; 821:152790. <https://doi.org/10.1016/j.scitotenv.2021.152790>.
38. Kotwa JD, Jamal AJ, Mbareche H *et al.* Surface and air contamination with severe acute respiratory syndrome coronavirus 2 from hospitalized coronavirus disease 2019 patients in Toronto, Canada, March–May 2020. *J Infect Dis* 2022; 225:768–76. <https://doi.org/10.1093/infdis/jiab578>.
39. Guadalupe JJ, Rojas MI, Pozo G *et al.* Presence of SARS-CoV-2 RNA on surfaces of public places and a transportation system located in a densely populated urban area in South America. *Viruses* 2022; 14:19. <https://doi.org/10.3390/v14010019>.
40. Santarpia JL, Rivera DN, Herrera VL *et al.* Aerosol and surface contamination of SARS-CoV-2 observed in quarantine and isolation care. *Sci Rep* 2020; 10:12732. <https://doi.org/10.1038/s41598-020-69286-3>.
41. Zhang X, Wu J, Smith LM *et al.* Monitoring SARS-CoV-2 in air and on surfaces and estimating infection risk in buildings and buses on a university campus. *J Expo Sci Environ Epidemiol* 2022; 32:751–8. <https://doi.org/10.1038/s41370-022-00442-9>.
42. Riddell S, Goldie S, Hill A *et al.* The effect of temperature on persistence of SARS-CoV-2 on common surfaces. *Virology* 2020; 17:145. <https://doi.org/10.1186/s12985-020-01418-7>.
43. Yu W, Huaiyu T, Li Z *et al.* Reduction of secondary transmission of SARS-CoV-2 in households by face mask use, disinfection and social distancing: a cohort study in Beijing. *China BMJ Glob Health* 2020; 5:e002794. <https://doi.org/10.1136/bmjgh-2020-002794>.
44. Morawska L, Cao J. Airborne transmission of SARS-CoV-2: the world should face the reality. *Environ Int* 2020; 139:105730. <https://doi.org/10.1016/j.envint.2020.105730>.
45. Shen J, Kong M, Dong B *et al.* Airborne transmission of SARS-CoV-2 in indoor environments: a comprehensive review. *Sci Technol Built Environ* 2021; 27:1331–67. <https://doi.org/10.1080/23744731.2021.1977693>.
46. Prentiss M, Chu A, Berggren KK. Finding the infectious dose for COVID-19 by applying an airborne-transmission model to Superspreader events. *PLoS One* 2022; 17:e0265816. <https://doi.org/10.1371/journal.pone.0265816>.
47. Pitol AK, Julian TR. Community transmission of SARS-CoV-2 by surfaces: risks and risk reduction strategies. *Environ Sci Technol Lett* 2021; 8:263–9. <https://doi.org/10.1021/acs.estlett.0c00966>.
48. Cherrie JW, Cherrie MPC, Smith A *et al.* Contamination of air and surfaces in workplaces with SARS-CoV-2 virus: a systematic review. *Ann Work Expo Health* 2021; 65:879–92. <https://doi.org/10.1093/annweh/wxab026>.
49. Chia PY, Coleman KK, Tan YK *et al.* Detection of air and surface contamination by SARS-CoV-2 in hospital rooms of infected patients. *Nat Commun* 2020; 11:2800. <https://doi.org/10.1038/s41467-020-16670-2>.
50. Geng Y, Wang Y. Stability and transmissibility of SARS-CoV-2 in the environment. *J Med Virol* 2023; 95:e28103. <https://doi.org/10.1002/jmv.28103>.
51. Pottage T, Garratt I, Onianwa O *et al.* A comparison of persistence of SARS-CoV-2 variants on stainless steel. *J Hosp Infect* 2021; 114:163–6. <https://doi.org/10.1016/j.jhin.2021.05.015>.
52. Liu J, Liu J, He Z *et al.* Duration of SARS-CoV-2 positive in quarantine room environments: a perspective analysis. *Int J Infect Dis* 2021; 105:68–74. <https://doi.org/10.1016/j.ijid.2021.02.025>.
53. Vass WB, Lednicky JA, Shankar SN *et al.* Viable SARS-CoV-2 Delta variant detected in aerosols in a residential setting with a self-isolating college student with COVID-19. *J Aerosol Sci* 2022; 165:106038. <https://doi.org/10.1016/j.jaerosci.2022.106038>.
54. Lednicky JA, Lauzardo M, Alam MM *et al.* Isolation of SARS-CoV-2 from the air in a car driven by a COVID patient with mild illness. *Int J Infect Dis* 2021; 108:212–6. <https://doi.org/10.1016/j.ijid.2021.04.063>.
55. Ratnesar-Shumate S, Bohannon K, Williams G *et al.* Comparison of the performance of aerosol sampling devices for measuring infectious SARS-CoV-2 aerosols. *Aerosol Sci Tech* 2021; 55:975–86. <https://doi.org/10.1080/02786826.2021.1910137>.
56. Maestre JP, Jarma D, Yu J-RF *et al.* Distribution of SARS-CoV-2 RNA signal in a home with COVID-19 positive occupants. *Sci Total Environ* 2021; 778:146201. <https://doi.org/10.1016/j.scitotenv.2021.146201>.
57. Glinert I, Ben-Shmuel A, Schwartz-Cohen M *et al.* Revisiting SARS-CoV-2 environmental contamination by patients with COVID-19: the omicron variant does not differ from previous strains. *Int J Infect Dis* 2022; 118:211–3. <https://doi.org/10.1016/j.ijid.2022.03.001>.
58. Chen J, Wang R, Gilby NB, Wei G-W. Omicron variant (B.1.1.529): infectivity, vaccine breakthrough, and antibody resistance. *J Chem Inf Model* 2022; 62:412–22. <https://doi.org/10.1021/acs.jcim.1c01451>.